Stress granule dysfunction via chromophore-associated light inactivation

Takumi Koizumi[1], Haruka Kawaguchi[1], Tsumugi Kurosaki[1], Akira Kitamura[2,3*]

[1]Laboratory of Molecular Cell Dynamics, Graduate School of Life Science, Hokkaido University, Sapporo, Japan

[2]Laboratory of Molecular Cell Dynamics, Faculty of Advanced Life Science, Hokkaido University, Sapporo, Japan

[3]PRIME, Japan Agency for Medical Research and Development, Chiyoda-ku, Tokyo, Japan

*** Correspondence:**
Akira Kitamura
akita@sci.hokudai.ac.jp
ORCiD ID: https://orcid.org/0000-0001-8357-8593

Keywords: stress granule, G3BP1, TDP-43, cell viability, chromophore-associated light inactivation

Abstract

Stress granules (SGs) are membraneless organelles composed of various proteins and RNAs that protect translation-associated machinery from harmful conditions during stress. However, the functional differences among SG compartments remain unclear. Here, we show that the spatial and temporal control of SG subcompartments by chromophore-associated light inactivation (CALI) using a genetically encoded red fluorescence protein (SuperNova-Red) as a photosensitizer leads to differences in cell viability during recovery from hyperosmotic stress and that the inactivation of the core phase in the SGs could be more critical than the shell phase. CALI delayed the disassembly kinetics of SGs during recovery from hyperosmotic stress. Consequently, CALI could inactivate the subcompartments of the SGs, and the cellular fate due to SGs could be analyzed. Furthermore, CALI is an effective spatiotemporal knockdown method for intracellular condensates/aggregates and contributes to the elucidation of membraneless organelles.

1 Introduction

Stress granules (SGs) are membraneless organelles; they are biomolecular condensates composed of proteins and RNAs that emerge in the cytoplasm under cellular stresses such as hyperosmotic, heat, and oxidative stress (1, 2). After being released from stress, the SGs are reversibly disassembled (1). Although the function of SGs remains elusive, they have long been proposed to play a role in protecting translation-associated RNAs from harmful conditions under stress because translation-associated proteins and RNAs, such as ribosomes, pre-translation complexes with mRNA, and various translation-associated RNA-binding proteins (RNPs), are widely sequestered into the SGs (3-5). Therefore, SGs are believed to play a cytoprotective role under stress conditions. SGs contain a biphasic structure with a stable “core” phase surrounded by a less concentrated “shell” phase (6). Ras-GTPase-activating protein SH3 domain-binding protein 1 (G3BP1) is an RNA-binding protein

37 essential for SG formation, which can primarily be found in the core phase (1, 2). Loss of G3BP1
38 increases the number of ubiquitinated proteins and toxic aggregates (7, 8) and inhibits the
39 proliferation of cancer cells (9). Transactivation response DNA/RNA-binding protein 43 kDa (TDP-
40 43) is an amyotrophic lateral sclerosis-associated aggregation-prone protein and a component of SGs.
41 One starting point for the pathological aggregation of TDP-43 is its localization to and interaction
42 with SG components in the shell phase (10). As the functional structure of SGs, the core phase is an
43 important scaffold for SG formation. The genetic depletion of endogenous G3BP1 reduces SG
44 formation efficiency (11). However, it is still unknown whether the loss of SG proteins in the shell
45 phase causes severe defects in the SGs. To elucidate the mechanisms underlying this issue, the
46 spatiotemporal inactivation of the shell phase, rather than the genetic knockout/knockdown of genes
47 of interest, is required because compartment-specific protein knockdown is not feasible with
48 traditional genetic methods.

49 Chromophore-assisted light inactivation (CALI) is used for the spatiotemporal inactivation of
50 specific compartments of live cells (12, 13). Absorption of light by the chromophore in phototoxic
51 photosensitizers produces reactive oxygen species (ROS), which, in turn, inactivates photosensitizer-
52 proximate biomolecules. Although various photosensitizers have been used, fluorescent protein-
53 based photosensitizers can be labeled at a defined molar ratio (e.g., 1:1) with the target protein,
54 expressed in cells via gene transfection, and localized to specific subcellular compartments (14).
55 SuperNova-Red (SNR) is a monomeric photosensitizer and a red fluorescent protein with high ROS
56 production (15). Therefore, we hypothesized that the spatiotemporal inactivation of SGs can be
57 achieved by tagging the SNR to specific proteins within specific compartments in the SGs under
58 stress.

59 In this report, we show how CALI changes the cell viability and kinetics of SG disassembly using
60 SNR to G3BP1 and TDP-43 in the SGs as targets during the recovery process after hyperosmotic
61 stress.

62 2 Materials and methods

63 *Plasmids*: To create the expression plasmids of proteins that SNR was tagged at the C-terminus of
64 G3BP1 and TDP-43, SNR DNA fragment (gift from Prof. T. Nagai) was inserted into the *Bam*HI and
65 *Not*I sites of pcDNA3.1(+) (Thermo Fisher Scientific, Waltham, MA, USA) (pcDNA-SNR). Next,
66 the DNA fragments of human TDP-43 obtained from the TDP-43 expression plasmid as previously
67 reported (16) and G3BP1 from Addgene (Clone#129339, Watertown, MA, USA) were inserted into
68 the *Hind*III and *Bam*HI sites of pcDNA-SNR (pTDP43-SNR and pG3BP1-SNR, respectively). To
69 create monomeric enhanced green fluorescent protein (meGFP)-tagged TDP-43 or G3BP1 expression
70 vectors, the DNA fragment of the SNR of pTDP43-SNR and pG3BP1-SNR was cut and substituted
71 with that of meGFP digested from pmeGFP-N1 (16) using the *Bam*HI and *Not*I sites (pTDP43-GFP
72 and pG3BP1-GFP, respectively). The expression plasmid for meGFP-tagged histone H2B (pBOS-
73 H2B-GFP) was the same as that used previously (16, 17).

74 *Cell Culture and Transfection*: Neuro-2a murine neuroblastoma (N2a) cells were obtained from the
75 American Type Culture Collection (ATCC; Manassas, VA, USA) and maintained in Dulbecco's
76 Modified Eagle Medium (DMEM) (D5796, Sigma-Aldrich, St. Louis, MO, USA) supplemented with
77 10% heat-inactivated fetal bovine serum (FBS) (12676029, Thermo Fisher Scientific), 100 U/mL
78 penicillin G (Sigma-Aldrich), and 0.1 mg/mL streptomycin (Sigma-Aldrich), as previously described
79 (16). One day before transfection, 2.0×10^5 N2a cells were transferred to a glass bottom dish (3910-
80 035, IWAKI-AGC Technoglass, Shizuoka, Japan). The mixture of expression plasmids was

transfected using Lipofectamine 2000 (Thermo Fisher Scientific) according to the manufacturer's protocol. Details on the amounts of the plasmids are described in the Supplementary Table. After 24 h of incubation, the spent medium was replaced with Opti-MEM I (Thermo Fisher Scientific) or Opti-MEM I containing 290 mM NaCl (hyperosmotic medium).

Stress granule formation, light irradiation, and time-lapse observation: To generate SGs under hyperosmotic stress, N2a cells were incubated in a hyperosmotic medium for 3 h. After the hyperosmotic medium was removed, the cells were washed thrice in Hank's balanced salt solution, and then the medium was exchanged with Opti-MEM I (recovery medium) containing 0.3 mM DRAQ7 (BioStatus, Leicestershire, UK) as an indicator for dead cells. After medium exchange, the glass-based dish was immediately placed on a microscope stage within 2 min. Light irradiation and time-lapse observations were performed using an Axioobserver Z1 inverted microscope (Carl Zeiss, Jena, Germany) equipped with an LSM510 META laser scanning confocal unit (Carl Zeiss), a C-Apochromat 40×/1.2NA W Korr. UV-VIS-IR water immersion objective (Carl Zeiss), laser sources, a mercury lamp, and a heat stage incubator (at 37°C supplemented with 5% CO_2). The field stop was set to a minimum. For CALI, cells 1–5 expressing SNR-tagged proteins were simultaneously irradiated with light from a mercury lamp through a 540–580 nm bandpass filter (ET560/40x; Chroma Technology Corporation, Bellows Falls, VT, USA) and a 585 nm dichroic mirror (T585lpxr; Chroma Technology Corporation) for 2 min. The aperture diaphragm was adjusted so that the light intensity was 0.9 mW just above the objective lens. After the CALI of SNR, bright-field and DRAQ7 fluorescence images of the irradiated cells were acquired at 30-minute intervals for up to 600 min (Supplementary Figure 1). The DRAQ7-stained cells were excited at 633 nm. The excitation and emission beams were split using a beam splitter (HFT405/488/543/633). Fluorescence was detected using photomultiplier tubes through a 650 nm long-pass filter (LP650). The diameter of the pinhole for DRAQ7 was 92 μm. The image size was 1024 × 1024 pixels and the zoom factor was 3. DRAQ7-positive cells were considered dead. To observe SG disassembly, GFP was excited at 488 nm. The excitation and emission beams were split using a beam splitter (HFT488/594). Fluorescence was detected using photomultiplier tubes through a 505–570 nm bandpass filter (BP505–570). The pinhole diameter was 72 μm, the image size was 1024 × 1024 pixels, and the zoom factor was 4. After light irradiation for CALI, bright-field and GFP fluorescence images of the irradiated cells were acquired at 30-minute intervals for up to 600 min.

Confocal microscopy: Image acquisition was performed using an inverted fluorescence microscope, Axioobserver Z1 (Carl Zeiss, Jena, Germany), combined with an LSM 510META system (Carl Zeiss), a C-Apochromat 40×/1.2NA W Korr. UV-VIS-IR water immersion objective (Carl Zeiss), laser sources, a mercury lamp, and a heat stage incubator (at 37°C supplemented with 5% CO_2). GFP and SNR were excited at 488 nm and 594 nm, respectively. The excitation and emission beams were split using a beam splitter (NFT488/594). Fluorescence was detected using photomultiplier tubes through a 615 nm long-pass filter (LP615). The diameter of the pinhole was 72 μm for GFP and 208 μm for SNR.

Statistical analyses: Student's t-tests were performed using Microsoft Excel. The generalized Wilcoxon test (Gehan-Breslow method) was performed using the Bell Curve for Excel software (Social Survey Research Information Co., Ltd., Tokyo, Japan).

3 Results

3.1 After CALI, SG-containing cells showed low viability during recovery from hyperosmotic stress

125 To demonstrate whether SGs play a cytoprotective role, we established a procedure to observe the
126 viability of cells expressing a protein target in CALI during the recovery period after hyperosmotic
127 stress caused by 290 mM NaCl (Supplementary Figure 1). Under this condition, SGs form in the
128 cytoplasm because their assembly and disassembly have previously been clarified under
129 hyperosmotic stress and after the recovery process (18). First, we tested whether the SNR monomers
130 induce cell death in the recovery medium after hyperosmotic stress. After light irradiation, no SNR
131 fluorescence was detected, indicating that SNR was efficiently photobleached (Supplemental Figure
132 2A). Photobleaching is important for ROS production from fluorophores (19). The viability of cells
133 expressing SNR monomers decreased to 86% at 600 min after the start of the time-lapse observation
134 (Supplemental Figure 2B), indicating that neither ROS from SNR monomers nor the cellular
135 recovery process from hyperosmotic stress caused cell death.

136 Next, as G3BP1 localizes in the core phase of SGs, we chose G3BP1 as a target for the
137 inactivation of SGs in CALI. Cytoplasmic SGs of G3BP1-SNR were observed in some of the cells
138 exposed to hyperosmotic stress; however, cells without SGs of G3BP1-SNR were also observed
139 (Figure 1A). Hence, we compared the proportion of surviving cells harboring SGs with that of cells
140 not harboring SGs during recovery from hyperosmotic stress. As negative controls, almost all cells
141 without light irradiation were alive regardless of G3BP1-SNR SG formation (green and orange lines,
142 Figure 1B), indicating that neither the recovery process from hyperosmotic stress nor time-lapse
143 observation affected the survival of the cells expressing G3BP1-SNR. In contrast, cells exposed to
144 hyperosmotic stress with light irradiation gradually died in both the SG-positive and SG-negative cell
145 groups during recovery from hyperosmotic stress. However, cells harboring SGs of G3BP1-SNR
146 died within a shorter time than those that did not (blue and magenta lines, Figure 1B). Therefore, we
147 successfully confirmed the reduction in cell viability induced by CALI in cells expressing G3BP1-
148 SNR, and that SG-positive cells were more likely to be affected by CALI-induced cell death than
149 SG-negative cells.

150 As TDP-43 localizes in the shell phase of SGs (10), we chose it as a target for the inactivation of
151 SGs in CALI. We also tracked cell viability after light irradiation using the same procedure as
152 G3BP1-SNR, where cells with and without TDP43-SNR SGs were observed (Figure 2A). Similar to
153 G3BP1-SNR-expressing cells, cell death was not observed in TDP43-SNR-expressing cells,
154 regardless of SGs, when no light was used as a negative control (green and orange lines, Figure 2B).
155 In contrast, significant cell death was observed in cells harboring SGs of TDP43-SNR; most cells that
156 did not harbor TDP43-SNR SGs remained alive (blue and magenta lines, Figure 2B). Furthermore, a
157 higher proportion of CALI-induced cell death was observed in cells expressing G3BP1-SNR than in
158 those expressing TDP43-SNR (Figure 3).

159 **3.2 CALI inhibits SG disassembly**

160 As SGs are gradually disassembled during recovery from hyperosmotic stress (20), we investigated
161 whether CALI-induced G3BP1 or TDP-43 inactivation in SGs affected the disassembly of SGs. To
162 observe the subcellular localization of G3BP1 or TDP-43 after the photobleaching of SNR for CALI,
163 N2a cells co-expressing meGFP-tagged and SNR-tagged G3BP1/TDP-43 were subjected to
164 hyperosmotic stress to form SGs in the cytoplasm, and then irradiated with light immediately after
165 replacement with the recovery medium. Immediately after light irradiation in CALI, the SNR
166 fluorescence completely disappeared; however, the subcellular localization of GFP-tagged G3BP1
167 and TDP-43 was not affected (Supplementary Figure 3). Next, the disassembly of G3BP1- and TDP-
168 43-containing SGs was observed using time-lapse fluorescence microscopy (Figure 4A). G3BP1-
169 containing SGs were gradually disassembled with and without light irradiation in the recovery

170 medium. However, in the light-irradiated cells, the SG disassembly speed was delayed up to ~270
171 min in the recovery medium, and the population of cells harboring SGs decreased to the same extent
172 with and without light irradiation (>300 min) (Figure 4B). The TDP-43-containing SGs with and
173 without light irradiation gradually disassembled at a similar speed in the recovery medium (Figure
174 4B). Although the disassembly speed of TDP-43-containing SGs in the recovery medium did not
175 differ with or without light irradiation up to ~270 min, its disassembly in light-irradiated cells did not
176 progress after its abundance was reduced to approximately 40% of the original; the remaining
177 proportion of SGs in light-irradiated cells was greater than that in non-irradiated cells (>350 min)
178 (Figure 4C). In summary, CALI inhibited SG disassembly.

179 **4 Discussion**

180 Here, we showed that CALI using SNR to target G3BP1 and TDP-43 in SGs increased cell death
181 (Figures 1–3) and inhibited SG disassembly (Figure 4). First, we determined the possible
182 mechanisms by which CALI inhibits SG disassembly. Light-irradiated SNR produces both
183 superoxide and singlet oxygen as ROS; however, the quantum yield of SNR to generate singlet
184 oxygen is approximately 15-fold higher than that to generate superoxide (19). The higher efficiency
185 of SNR in generating singlet oxygen compared to superoxide is similar to other red fluorescent
186 proteins, such as mCherry (21) and KillerRed (22) but the highest among these proteins (15, 19). The
187 lifetime of singlet oxygen in water was reported at 3.7 μs (23). However, the travel distance of singlet
188 oxygen in cells is believed to be less than 2 nm because singlet oxygen reacts with water and other
189 biomolecules (24); hence, singlet oxygen can spread only within the local environment (25). Because
190 the short diameter of the fluorescent protein-conserved β-barrel of SNR is approximately 1.3 nm
191 (15), the singlet oxygen produced from SNR is consumed by biomolecules close to the outside of the
192 β-barrel.

193 Singlet oxygen damages proteins, peptides, and nucleic acids in various ways (26-30). In
194 proteins and peptides, singlet oxygen can react with the side chains of amino acids (e.g., Trp, Tyr,
195 His, Met, and Cys), resulting in the chemical modification of these amino acids, backbone
196 fragmentation, cross-linking, and subsequent aggregation (26, 31). In nucleic acids, guanosine is a
197 major oxidization target of singlet oxygen (29, 30). Because SGs are densely packed with various
198 proteins and RNAs (1, 2), singlet oxygen generated from G3BP1-SNR or TDP43-SNR may act on
199 the proteins and RNAs in the SGs, leading to side chain modifications, backbone fragmentations, and
200 cross-linking of SG components in the phase where SNR-tagged proteins are localized. These effects
201 do not produce an immediate change or instantaneous disappearance of SGs (Supplementary Figure
202 3); however, they inhibit SG disassembly (Figure 4B). As previously reported, the most easily
203 interpreted cause of difficulty in SG disassembly is intermolecular cross-linking (32-34). Another
204 possibility is that molecular chaperones such as HSP70 are incorporated in the SGs to protect and
205 possibly repair proteins that unfold during various types of stress and are required for the
206 disassembly of SGs (3). Inactivation of such molecular chaperones by CALI would cause defects in
207 SG disassembly. As the abundance, conformations, modifications, and interactions of RNA may
208 control the assembly and disassembly of SGs (1, 35), singlet oxygen-induced guanosine oxygenation
209 in RNA may retard the SG disassembly process.

210 Because cross-linking is a covalent bond, the dissociation of biomolecules is less likely to occur.
211 Interestingly, the disassembly kinetics differed between G3BP1 and TDP-43 (Figure 4B). As G3BP1
212 and TDP-43 localize to different phases in the SG (core and shell, respectively), CALI may affect the
213 disassembly process in each phase. As TDP-43 is localized in the shell, the outer phase of the SGs,
214 TDP-43 may be released not as a single molecule but as an oligomeric or multimeric unit, likely with

215 other SG components. However, the population of TDP-43 cross-linked with molecules that are static
216 in the SG may remain inside the SGs. In contrast, because G3BP1 localizes to the core phase of the
217 SGs, when the SG itself collapses, it is likely to dissociate less if it is cross-linked. However, light-
218 irradiated G3BP1-harboring SGs disassembled even after a delay, so there may be a repair system for
219 cross-linked species during SG disassembly. Although singlet oxygen was artificially generated from
220 SNR in this experiment, singlet oxygen and other ROS can be generated by intracellular redox
221 reactions in physiological environments (36). Singlet oxygen and other ROS generated in
222 physiological states form intermolecular cross-links in SGs. In other words, this study attempted to
223 mimic the effects of singlet oxygen-promoted inactivation of intracellular structures such as SGs.

224 Next, we discuss the influence of CALI outside the SGs (i.e., in the cytoplasm and nucleus). The
225 G3BP1-SNR and TDP-43-SNR used in this study were localized not only in the SGs but also in the
226 cytoplasm and nucleus. Because whole cells were irradiated with light, ROS may have been
227 produced in the cytoplasm and nucleus. Our results showed that cell death was more pronounced
228 after CALI in SG-positive cells for both G3BP1-SNR and TDP-43-SNR (Figures 1–3), suggesting
229 that SG inactivation was more strongly associated with cell death than defects in these proteins
230 localized in the cytoplasm or nucleus. However, CALI in cells not harboring SGs of G3BP1-SNR
231 also induced cell death (Figure 1), suggesting that the inactivation of G3BP1 in the cytoplasm and
232 nucleus may be involved in cell death. Loss of G3BP1 increases protein ubiquitination and the
233 aggregation of toxic huntingtin (7, 8) and diminishes the proliferation of breast cancer cells (9); the
234 inactivation of G3BP1 by CALI likely leads to proteostasis dysregulation and eventual cell death. In
235 contrast, the loss of TDP-43 leads to various cellular dysfunctions, such as the misregulation of RNA
236 splicing and its quality control, mitochondrial dysfunction, and cell death (37-40). However, cell
237 death during TDP-43 knockdown was observed at approximately 120 h after siRNA introduction
238 (40). This suggests that cell death by TDP-43 depletion may not be an acute response but rather via
239 the accumulation of various dysfunctions. CALI of TDP43-SNR in cells not harboring SGs did not
240 result in a dramatic increase in cell death (Figure 2B), consistent with the slow rate of cell death
241 observed in TDP43-depleted cells. This supports the specificity of CALI for the protein of interest
242 and its localization.

243 Finally, we discuss the possible mechanisms of cell death induced by CALI in SGs. SGs
244 attenuate apoptotic cell death via p53 inhibition and the recruitment of ROCK1 and RACK1 to SGs
245 (41-43). SG formation regulates several canonical signaling pathways (such as NF-κB, mTORC1,
246 and PKR) and pro-survival functions during the acute stress response (1, 4). The dysfunction of SGs
247 induced by CALI may reactivate transiently inhibited apoptotic signaling pathways. The CALI-
248 induced aberrant RNA in the SGs may disturb cellular functions. mRNA translation is stalled as a
249 pre-initiation complex in SGs, as translation is traditionally considered silent during SG formation
250 (1). Although some mRNAs are translationally silent, a host of RNA molecules undergo translation
251 in SGs (44). Therefore, the translation dysfunction required for stress recovery is delayed by aberrant
252 RNA induced by CALI in the SGs, leading to cell death.

253 Consequently, here, we showed that CALI of two SG components (G3BP1 and TDP-43) using
254 SNR retarded SG disassembly and led to cell death. These results suggest that CALI can inactivate
255 various intracellular condensates composed of proteins and RNA in a spatiotemporally controlled
256 manner, and the subsequent cellular fate can be analyzed. Furthermore, we believe that CALI is an
257 effective method that contributes to identifying intercellular condensates/aggregates as hubs
258 controlling signal transduction. However, the molecular mechanism of inactivation by CALI remains
259 unknown, and its identification remains an important open question.

5 Conflict of Interest

The authors declare no conflicts of interest.

6 Author Contributions

TKo: Methodology, Formal Analysis; HK: Methodology, Formal Analysis; TKu: Methodology; AK: Writing – original draft, review, editing, Conceptualization, Methodology, Project administration.

7 Funding

This research was funded by the Japan Agency for Medical Research and Development (AMED), grant numbers JP23gm6410028, JP22ym0126814, and JP23ym0126801; the Japan Society for the Promotion of Science (JSPS), grant number 22H04826, 22H02578, and 22K19886; the Nakatani Foundation for Advancement of Measuring Technologies in Biomedical Engineering; the Hagiwara Foundation; the Hoansha Foundation; the Northern Advancement Center for Science & Technology (NOASTEC) for AK; and the Hokkaido University Office for Developing Future Research Leaders (L-Station).

8 Acknowledgments

We would like to thank Ms. Asuka Murata for technical support and Dr. Takeharu Nagai for generously providing us with a plasmid vector for SuperNova-Red.

9 Figure legends

Figure 1. Cell viability after chromophore-associated light inactivation (CALI) targeting G3BP1 in cells recovering from hyperosmotic stress. (A) Fluorescence images of SG-positive and SG-negative cells expressing SuperNova-Red (SNR)-tagged G3BP1 (G3BP1-SNR; magenta) and Histon H2B-GFP (green) before light irradiation for CALI. (B) Time-course cell viability plot (600 min) in the recovery medium after hyperosmotic stress with or without light irradiation for CALI (20 cells). *P*-values were obtained using the generalized Wilcoxon test (Gehan-Breslow method). ###$p < 0.001$ (compared to the group without light irradiation); **$p < 0.01$ between the lines; NS, not significant ($p \geq 0.05$).

Figure 2. Cell viability after chromophore-associated light inactivation (CALI) targeting TDP-43 in cells recovering from hyperosmotic stress. (A) Fluorescence images of SG-positive and SG-negative cells expressing SuperNova-Red (SNR)-tagged TDP-43 (TDP43-SNR; magenta) and Histon H2B-GFP (green) before light irradiation for CALI. (B) Time-course cell viability plot (600 min) in the recovery medium after hyperosmotic stress with or without light irradiation for CALI (20 cells). *P*-values were obtained using the generalized Wilcoxon test (Gehan-Breslow method). ##$p < 0.01$ (compared to the group without light irradiation); *$p < 0.05$ between the lines; NS, not significant ($p \geq 0.05$).

Figure 3. Comparison of cell viability after chromophore-associated light inactivation (CALI) between G3BP1 and TDP-43 in cells recovering from hyperosmotic stress. The plot lines are derived from the data shown in Figures 1B and 2B (20 cells). *P*-values were obtained using the generalized Wilcoxon test (Gehan-Breslow method). **$p < 0.01$ between the lines.

Figure 4. Disassembly of SGs containing G3BP1-GFP or TDP43-GFP after chromophore-associated light inactivation (CALI) targeting G3BP1-SNR or TDP43-SNR, respectively. (A) Time-lapse observation of cells harboring SGs of G3BP1-GFP or TDP43-GFP with (+) or without (-) light irradiation. (B) Plot showing the decrease in the normalized number of SGs containing G3BP1-GFP with (magenta) or without (green) light irradiation (mean ± 95%CI; 15 cells). *P*-values were obtained using Student's t-test. $*p < 0.05$ at the time indicated on the lines. (C) Plot showing the decrease in the normalized number of SGs containing TDP43-GFP with (magenta) or without (green) light irradiation (mean ± 95%CI; 15 cells). *P*-values were obtained using Student's t-test. $*p < 0.05$ at the indicated time points.

Figure 5. The possible mechanism of internal damage in SGs caused by light irradiation.

10 References

1. D. Campos-Melo, Z. C. E. Hawley, C. A. Droppelmann and M. J. Strong: The Integral Role of RNA in Stress Granule Formation and Function. *Front Cell Dev Biol*, 9, 621779 (2021) doi:10.3389/fcell.2021.621779

2. D. S. W. Protter and R. Parker: Principles and Properties of Stress Granules. *Trends Cell Biol*, 26(9), 668-679 (2016) doi:10.1016/j.tcb.2016.05.004

3. D. Tauber, G. Tauber and R. Parker: Mechanisms and Regulation of RNA Condensation in RNP Granule Formation. *Trends Biochem Sci*, 45(9), 764-778 (2020) doi:10.1016/j.tibs.2020.05.002

4. H. Zhou, J. Luo, K. Mou, L. Peng, X. Li, Y. Lei, J. Wang, S. Lin, Y. Luo and L. Xiang: Stress granules: functions and mechanisms in cancer. *Cell Biosci*, 13(1), 86 (2023) doi:10.1186/s13578-023-01030-6

5. S. Das, L. Santos, A. V. Failla and Z. Ignatova: mRNAs sequestered in stress granules recover nearly completely for translation. *RNA Biol*, 19(1), 877-884 (2022) doi:10.1080/15476286.2022.2094137

6. J. R. Wheeler, T. Matheny, S. Jain, R. Abrisch and R. Parker: Distinct stages in stress granule assembly and disassembly. *Elife*, 5 (2016) doi:10.7554/eLife.18413

7. S. Anisimov, M. Takahashi, T. Kakihana, Y. Katsuragi, H. Kitaura, L. Zhang, A. Kakita and M. Fujii: G3BP1 inhibits ubiquitinated protein aggregations induced by p62 and USP10. *Sci Rep*, 9(1), 12896 (2019) doi:10.1038/s41598-019-46237-1

8. R. Gutierrez-Garcia, S. Koyuncu, F. Hommen, S. Bilican, H. J. Lee, A. Fatima and D. Vilchez: G3BP1-dependent mechanism suppressing protein aggregation in Huntington's models and its demise upon stress granule assembly. *Hum Mol Genet*, 32(10), 1607-1621 (2023) doi:10.1093/hmg/ddac304

9. S. Liu, S. Tian, T. Lin, X. He, J. Eze Ideozu, R. Wang, Y. Wang, D. Yue and H. Geng: G3BP1 regulates breast cancer cell proliferation and metastasis by modulating PKCzeta. *Front Genet*, 13, 1034889 (2022) doi:10.3389/fgene.2022.1034889

10. B. Wolozin and P. Ivanov: Stress granules and neurodegeneration. *Nat Rev Neurosci*, 20(11), 649-666 (2019) doi:10.1038/s41583-019-0222-5

11. P. Yang, C. Mathieu, R. M. Kolaitis, P. Zhang, J. Messing, U. Yurtsever, Z. Yang, J. Wu, Y. Li, Q. Pan, J. Yu, E. W. Martin, T. Mittag, H. J. Kim and J. P. Taylor: G3BP1 Is a Tunable Switch that Triggers Phase Separation to Assemble Stress Granules. *Cell*, 181(2), 325-345 e28 (2020) doi:10.1016/j.cell.2020.03.046

339 12. T. Surrey, M. B. Elowitz, P. E. Wolf, F. Yang, F. Nedelec, K. Shokat and S. Leibler:
340 Chromophore-assisted light inactivation and self-organization of microtubules and motors. *Proc Natl*
341 *Acad Sci U S A*, 95(8), 4293-8 (1998) doi:10.1073/pnas.95.8.4293

342 13. M. E. Bulina, D. M. Chudakov, O. V. Britanova, Y. G. Yanushevich, D. B. Staroverov, T. V.
343 Chepurnykh, E. M. Merzlyak, M. A. Shkrob, S. Lukyanov and K. A. Lukyanov: A genetically
344 encoded photosensitizer. *Nat Biotechnol*, 24(1), 95-9 (2006) doi:10.1038/nbt1175

345 14. K. Jacobson, Z. Rajfur, E. Vitriol and K. Hahn: Chromophore-assisted laser inactivation in
346 cell biology. *Trends Cell Biol*, 18(9), 443-50 (2008) doi:10.1016/j.tcb.2008.07.001

347 15. K. Takemoto, T. Matsuda, N. Sakai, D. Fu, M. Noda, S. Uchiyama, I. Kotera, Y. Arai, M.
348 Horiuchi, K. Fukui, T. Ayabe, F. Inagaki, H. Suzuki and T. Nagai: SuperNova, a monomeric
349 photosensitizing fluorescent protein for chromophore-assisted light inactivation. *Sci Rep*, 3, 2629
350 (2013) doi:10.1038/srep02629

351 16. A. Kitamura, Y. Nakayama, A. Shibasaki, A. Taki, S. Yuno, K. Takeda, M. Yahara, N.
352 Tanabe and M. Kinjo: Interaction of RNA with a C-terminal fragment of the amyotrophic lateral
353 sclerosis-associated TDP43 reduces cytotoxicity. *Sci Rep*, 6, 19230 (2016) doi:10.1038/srep19230

354 17. T. Kanda, K. F. Sullivan and G. M. Wahl: Histone-GFP fusion protein enables sensitive
355 analysis of chromosome dynamics in living mammalian cells. *Curr Biol*, 8(7), 377-85 (1998)
356 doi:10.1016/s0960-9822(98)70156-3

357 18. A. Kitamura, S. Oasa, H. Kawaguchi, M. Osaka, V. Vukojevic and M. Kinjo: Increased
358 intracellular crowding during hyperosmotic stress. *Sci Rep*, 13(1), 11834 (2023) doi:10.1038/s41598-
359 023-39090-w

360 19. J. O. Onukwufor, A. J. Trewin, T. M. Baran, A. Almast, T. H. Foster and A. P. Wojtovich:
361 Quantification of reactive oxygen species production by the red fluorescent proteins KillerRed,
362 SuperNova and mCherry. *Free Radic Biol Med*, 147, 1-7 (2020)
363 doi:10.1016/j.freeradbiomed.2019.12.008

364 20. E. M. Hock, Z. Maniecka, M. Hruska-Plochan, S. Reber, F. Laferriere, M. K. S. Sahadevan,
365 H. Ederle, L. Gittings, L. Pelkmans, L. Dupuis, T. Lashley, M. D. Ruepp, D. Dormann and M.
366 Polymenidou: Hypertonic Stress Causes Cytoplasmic Translocation of Neuronal, but Not Astrocytic,
367 FUS due to Impaired Transportin Function. *Cell Rep*, 24(4), 987-1000 e7 (2018)
368 doi:10.1016/j.celrep.2018.06.094

369 21. N. C. Shaner, R. E. Campbell, P. A. Steinbach, B. N. Giepmans, A. E. Palmer and R. Y.
370 Tsien: Improved monomeric red, orange and yellow fluorescent proteins derived from Discosoma sp.
371 red fluorescent protein. *Nat Biotechnol*, 22(12), 1567-72 (2004) doi:10.1038/nbt1037

372 22. M. E. Bulina, K. A. Lukyanov, O. V. Britanova, D. Onichtchouk, S. Lukyanov and D. M.
373 Chudakov: Chromophore-assisted light inactivation (CALI) using the phototoxic fluorescent protein
374 KillerRed. *Nat Protoc*, 1(2), 947-53 (2006) doi:10.1038/nprot.2006.89

375 23. M. Bregnhoj, M. Westberg, F. Jensen and P. R. Ogilby: Solvent-dependent singlet oxygen
376 lifetimes: temperature effects implicate tunneling and charge-transfer interactions. *Phys Chem Chem*
377 *Phys*, 18(33), 22946-61 (2016) doi:10.1039/c6cp01635a

378 24. M. Klaper, W. Fudickar and T. Linker: Role of Distance in Singlet Oxygen Applications: A
379 Model System. *J Am Chem Soc*, 138(22), 7024-9 (2016) doi:10.1021/jacs.6b01555

380 25. M. K. Kuimova, G. Yahioglu and P. R. Ogilby: Singlet oxygen in a cell: spatially dependent
381 lifetimes and quenching rate constants. *J Am Chem Soc*, 131(1), 332-40 (2009)
382 doi:10.1021/ja807484b

383 26. D. G. Jay: Selective destruction of protein function by chromophore-assisted laser
384 inactivation. *Proc Natl Acad Sci U S A*, 85(15), 5454-8 (1988) doi:10.1073/pnas.85.15.5454

385 27. Y. Sano, W. Watanabe and S. Matsunaga: Chromophore-assisted laser inactivation--towards a
386 spatiotemporal-functional analysis of proteins, and the ablation of chromatin, organelle and cell
387 function. *J Cell Sci*, 127(Pt 8), 1621-9 (2014) doi:10.1242/jcs.144527

388 28. K. Takemoto, H. Iwanari, H. Tada, K. Suyama, A. Sano, T. Nagai, T. Hamakubo and T.
389 Takahashi: Optical inactivation of synaptic AMPA receptors erases fear memory. *Nat Biotechnol*,
390 35(1), 38-47 (2017) doi:10.1038/nbt.3710

391 29. J. L. Ravanat and E. Dumont: Reactivity of Singlet Oxygen with DNA, an Update.
392 *Photochem Photobiol*, 98(3), 564-571 (2022) doi:10.1111/php.13581

393 30. L. F. Agnez-Lima, J. T. Melo, A. E. Silva, A. H. Oliveira, A. R. Timoteo, K. M. Lima-Bessa,
394 G. R. Martinez, M. H. Medeiros, P. Di Mascio, R. S. Galhardo and C. F. Menck: DNA damage by
395 singlet oxygen and cellular protective mechanisms. *Mutat Res Rev Mutat Res*, 751(1), 15-28 (2012)
396 doi:10.1016/j.mrrev.2011.12.005

397 31. M. J. Davies: Singlet oxygen-mediated damage to proteins and its consequences. *Biochem*
398 *Biophys Res Commun*, 305(3), 761-70 (2003) doi:10.1016/s0006-291x(03)00817-9

399 32. E. Fuentes-Lemus, P. Hagglund, C. Lopez-Alarcon and M. J. Davies: Oxidative Crosslinking
400 of Peptides and Proteins: Mechanisms of Formation, Detection, Characterization and Quantification.
401 *Molecules*, 27(1) (2021) doi:10.3390/molecules27010015

402 33. Y. Furukawa, R. Fu, H. X. Deng, T. Siddique and T. V. O'Halloran: Disulfide cross-linked
403 protein represents a significant fraction of ALS-associated Cu, Zn-superoxide dismutase aggregates
404 in spinal cords of model mice. *Proc Natl Acad Sci U S A*, 103(18), 7148-53 (2006)
405 doi:10.1073/pnas.0602048103

406 34. A. Kitamura, N. Inada, H. Kubota, G. Matsumoto, M. Kinjo, R. I. Morimoto and K. Nagata:
407 Dysregulation of the proteasome increases the toxicity of ALS-linked mutant SOD1. *Genes Cells*,
408 19(3), 209-24 (2014) doi:10.1111/gtc.12125

409 35. M. Garcia-Jove Navarro, S. Kashida, R. Chouaib, S. Souquere, G. Pierron, D. Weil and Z.
410 Gueroui: RNA is a critical element for the sizing and the composition of phase-separated RNA-
411 protein condensates. *Nat Commun*, 10(1), 3230 (2019) doi:10.1038/s41467-019-11241-6

412 36. M. Herb, A. Gluschko and M. Schramm: Reactive Oxygen Species: Not Omnipresent but
413 Important in Many Locations. *Front Cell Dev Biol*, 9, 716406 (2021) doi:10.3389/fcell.2021.716406

414 37. M. Briese, L. Saal-Bauernschubert, P. Luningschror, M. Moradi, B. Dombert, V. Surrey, S.
415 Appenzeller, C. Deng, S. Jablonka and M. Sendtner: Loss of Tdp-43 disrupts the axonal
416 transcriptome of motoneurons accompanied by impaired axonal translation and mitochondria
417 function. *Acta Neuropathol Commun*, 8(1), 116 (2020) doi:10.1186/s40478-020-00987-6

418 38. F. C. Fiesel, C. Schurr, S. S. Weber and P. J. Kahle: TDP-43 knockdown impairs neurite
419 outgrowth dependent on its target histone deacetylase 6. *Mol Neurodegener*, 6, 64 (2011)
420 doi:10.1186/1750-1326-6-64

421 39. M. Polymenidou, C. Lagier-Tourenne, K. R. Hutt, S. C. Huelga, J. Moran, T. Y. Liang, S. C.
422 Ling, E. Sun, E. Wancewicz, C. Mazur, H. Kordasiewicz, Y. Sedaghat, J. P. Donohue, L. Shiue, C. F.

423 Bennett, G. W. Yeo and D. W. Cleveland: Long pre-mRNA depletion and RNA missplicing
424 contribute to neuronal vulnerability from loss of TDP-43. *Nat Neurosci*, 14(4), 459-68 (2011)
425 doi:10.1038/nn.2779

426 40. M. Yahara, A. Kitamura and M. Kinjo: U6 snRNA expression prevents toxicity in TDP-43-
427 knockdown cells. *PLoS One*, 12(11), e0187813 (2017) doi:10.1371/journal.pone.0187813

428 41. N. P. Tsai and L. N. Wei: RhoA/ROCK1 signaling regulates stress granule formation and
429 apoptosis. *Cell Signal*, 22(4), 668-75 (2010) doi:10.1016/j.cellsig.2009.12.001

430 42. Y. J. Park, D. W. Choi, S. W. Cho, J. Han, S. Yang and C. Y. Choi: Stress Granule Formation
431 Attenuates RACK1-Mediated Apoptotic Cell Death Induced by Morusin. *Int J Mol Sci*, 21(15)
432 (2020) doi:10.3390/ijms21155360

433 43. C. Mao, X. Wang, Y. Liu, M. Wang, B. Yan, Y. Jiang, Y. Shi, Y. Shen, X. Liu, W. Lai, R.
434 Yang, D. Xiao, Y. Cheng, S. Liu, H. Zhou, Y. Cao, W. Yu, K. Muegge, H. Yu and Y. Tao: A
435 G3BP1-Interacting lncRNA Promotes Ferroptosis and Apoptosis in Cancer via Nuclear Sequestration
436 of p53. *Cancer Res*, 78(13), 3484-3496 (2018) doi:10.1158/0008-5472.CAN-17-3454

437 44. D. Mateju, B. Eichenberger, F. Voigt, J. Eglinger, G. Roth and J. A. Chao: Single-Molecule
438 Imaging Reveals Translation of mRNAs Localized to Stress Granules. *Cell*, 183(7), 1801-1812 e13
439 (2020) doi:10.1016/j.cell.2020.11.010

440

Figure 1

(A)

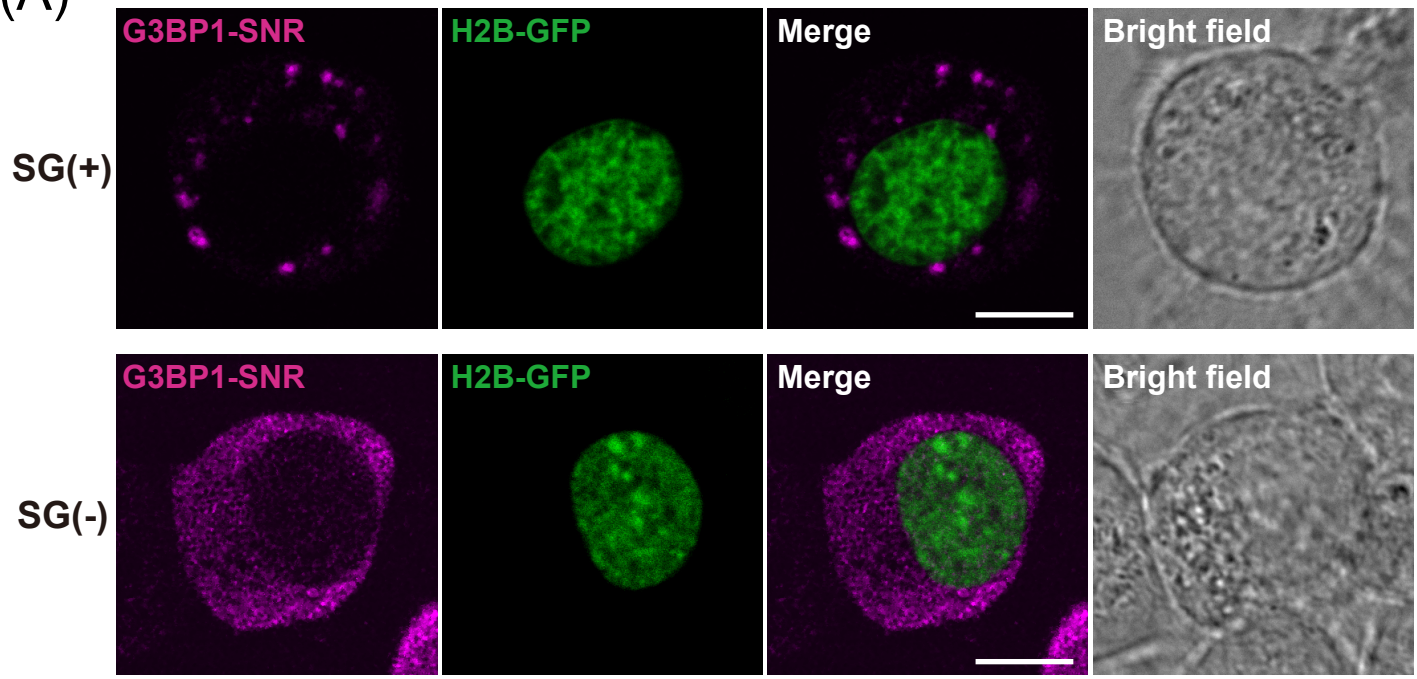
G3BP1-SNR
H2B-GFP
Merge
Bright field
SG(+)
SG(-)

(B)

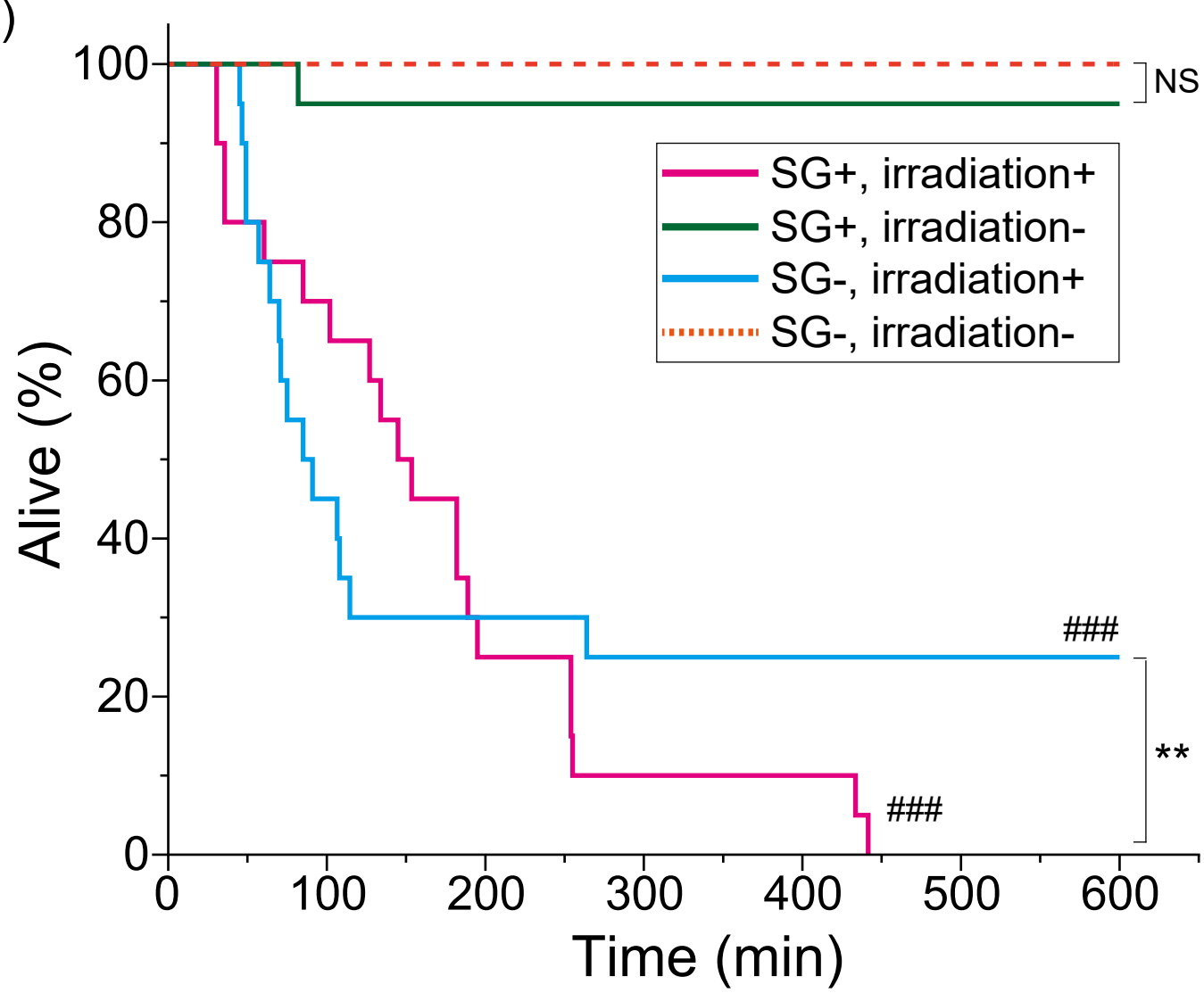
Alive (%)
Time (min)
0
20
40
60
80
100
0
100
200
300
400
500
600
SG+, irradiation+
SG+, irradiation-
SG-, irradiation+
SG-, irradiation-
NS
**
###
###

Figure 2

(A)

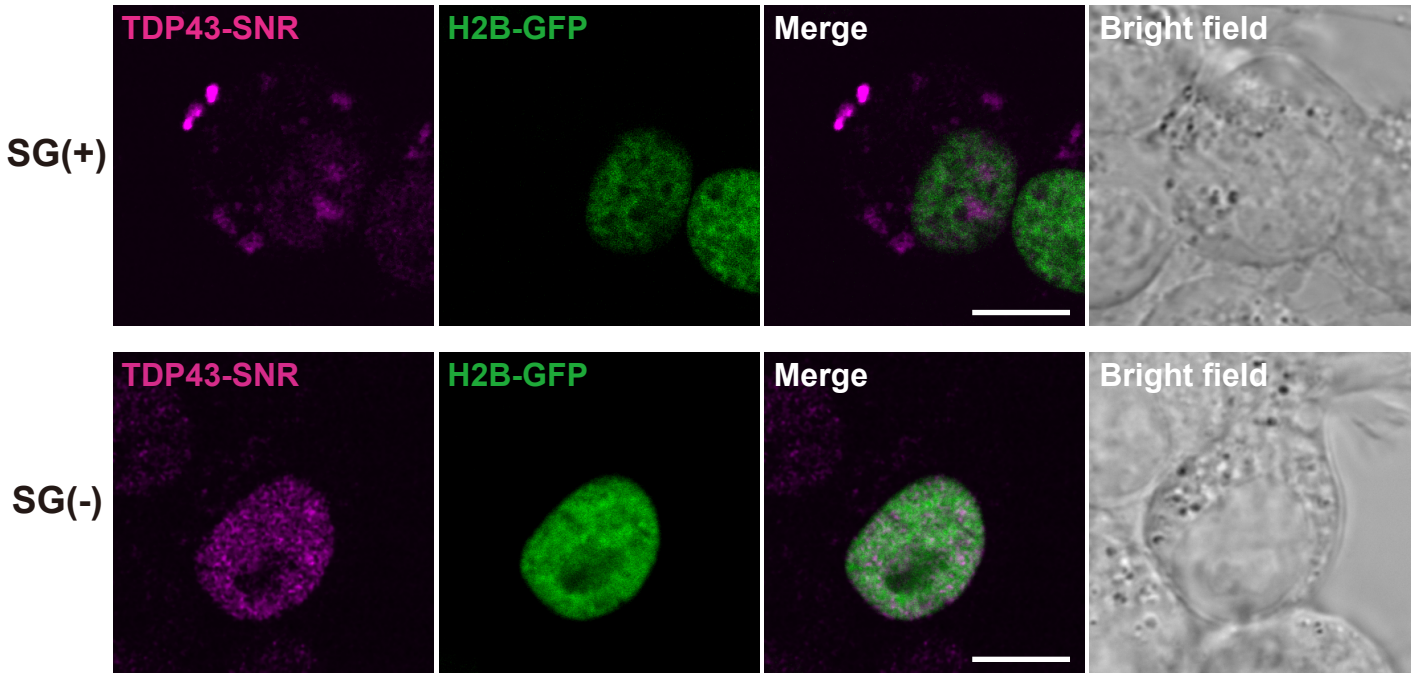
TDP43-SNR
H2B-GFP
Merge
Bright field
SG(+)
SG(-)

(B)

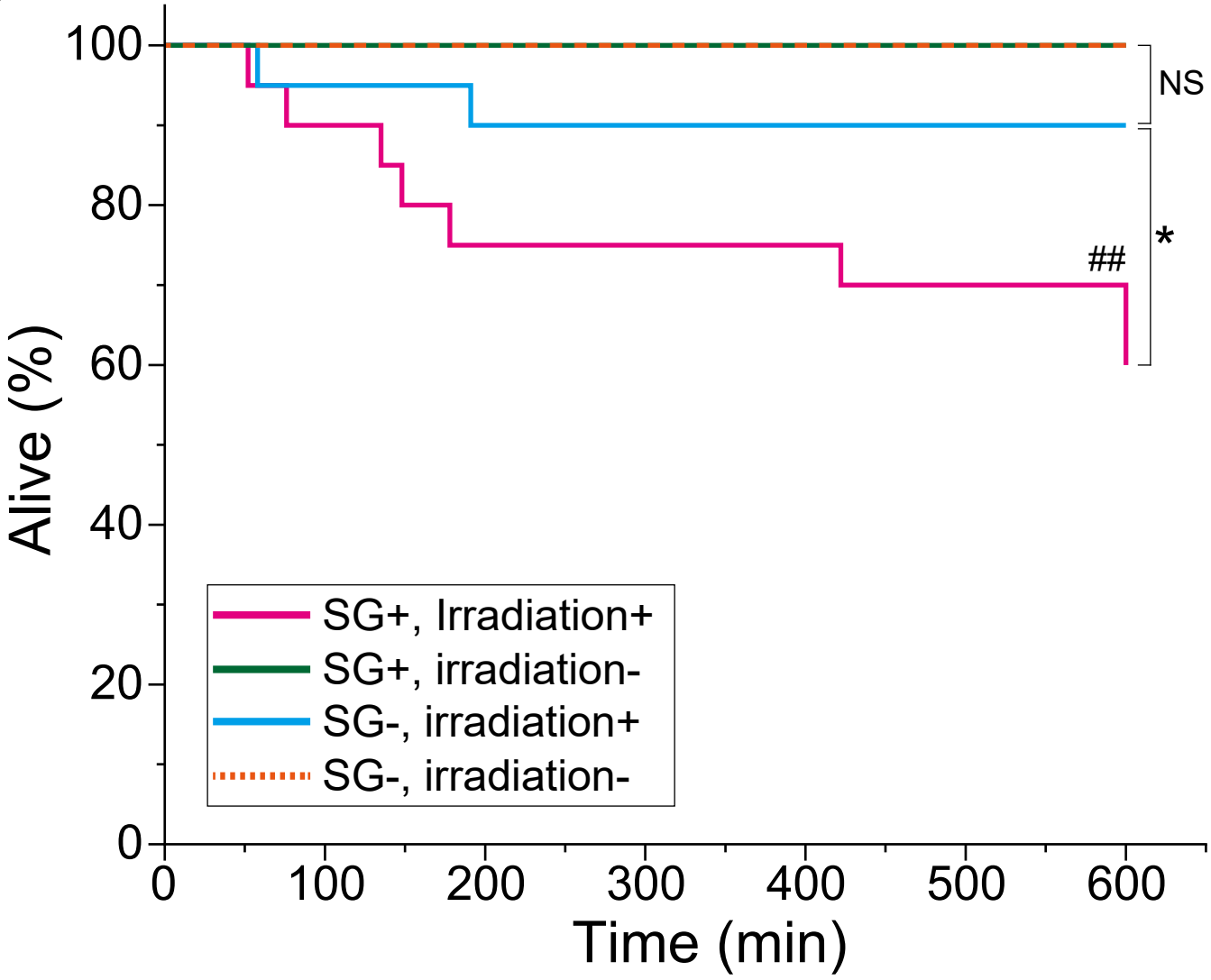
Alive (%)
Time (min)
0
20
40
60
80
100
0
100
200
300
400
500
600
NS
*
##
SG+, Irradiation+
SG+, irradiation-
SG-, irradiation+
SG-, irradiation-

Figure 3

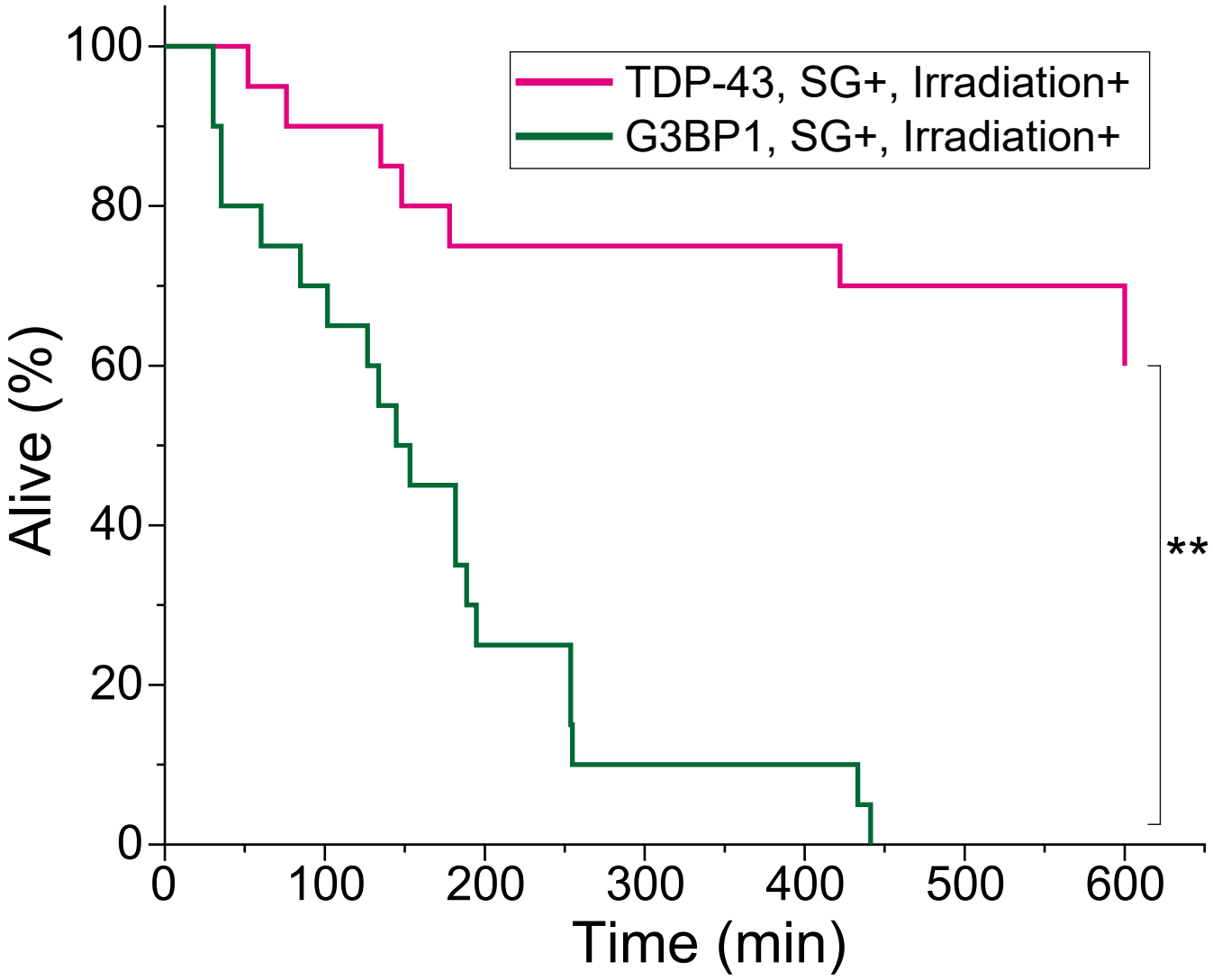
TDP-43, SG+, Irradiation+
G3BP1, SG+, Irradiation+
Alive (%)
100
80
60
40
20
0
0
100
200
300
400
500
600
Time (min)
**

Figure 4

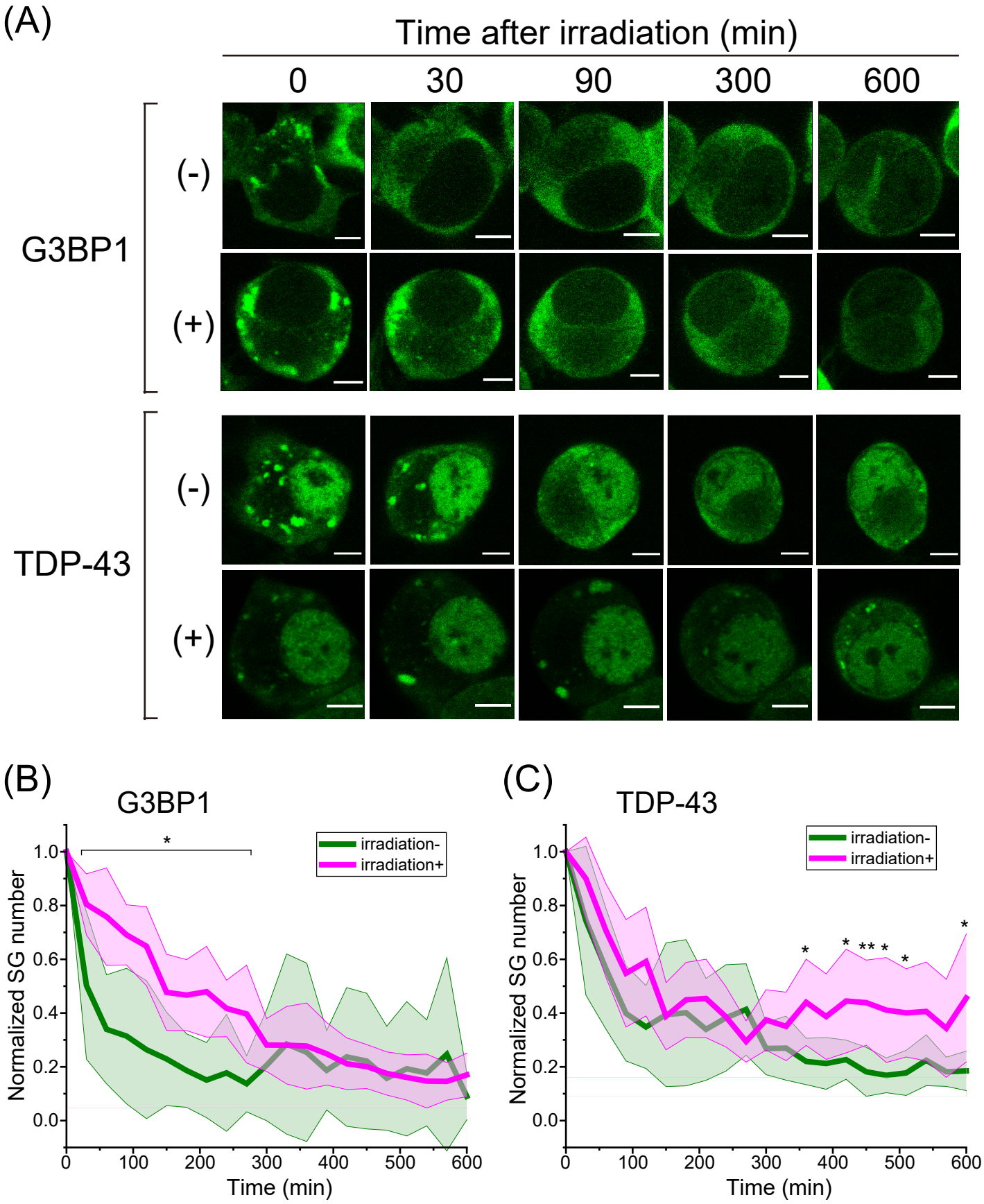
(A)
Time after irradiation (min)
0
30
90
300
600
G3BP1
(-)
(+)
TDP-43
(-)
(+)
(B)
G3BP1
irradiation-
irradiation+
Normalized SG number
Time (min)
(C)
TDP-43
irradiation-
irradiation+
Normalized SG number
Time (min)

Figure 5

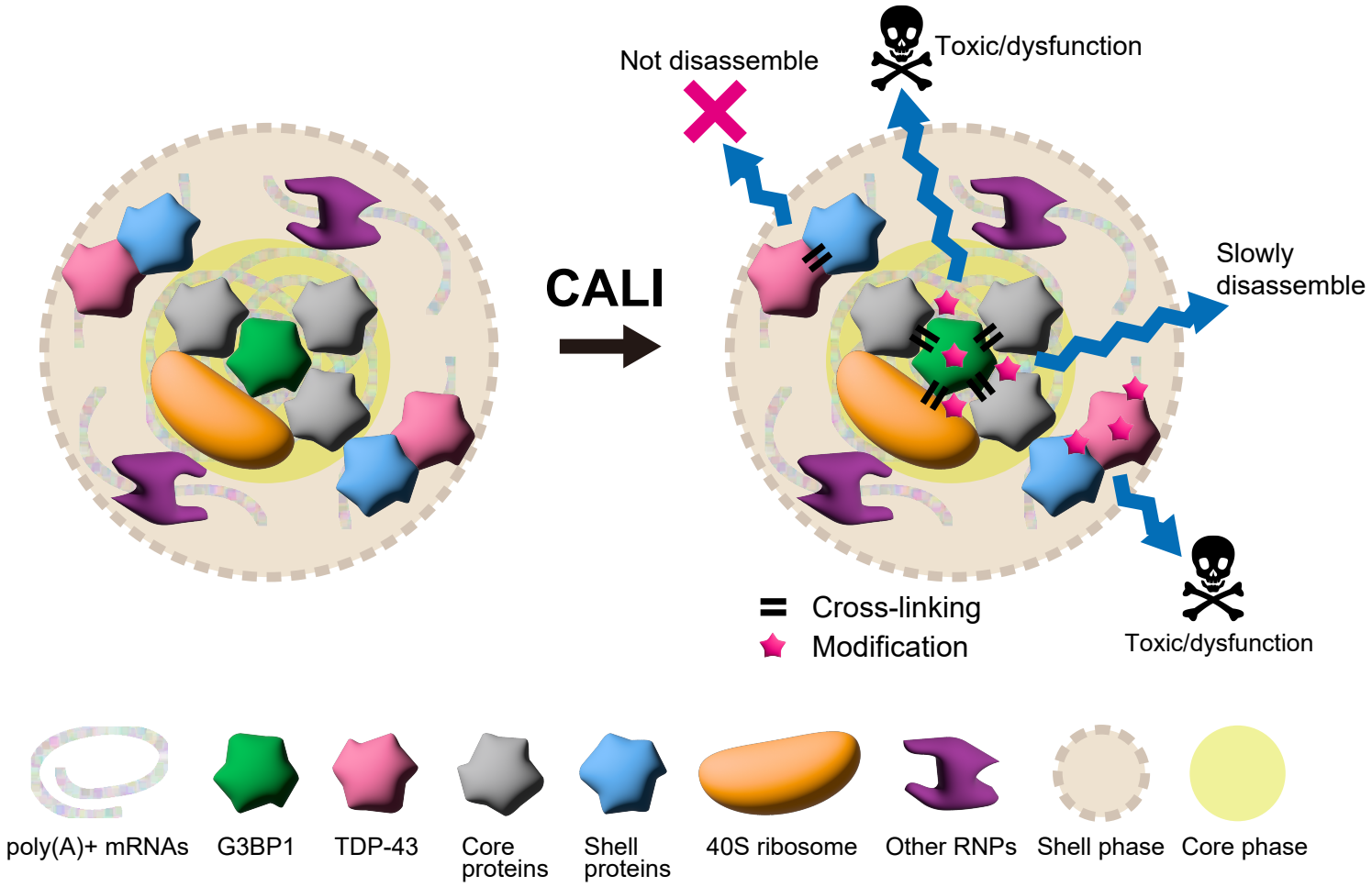
Not disassemble
Toxic/dysfunction
CALI
Slowly disassemble
Cross-linking
Modification
Toxic/dysfunction
poly(A)+ mRNAs
G3BP1
TDP-43
Core proteins
Shell proteins
40S ribosome
Other RNPs
Shell phase
Core phase